

MOST PROBABLE PATHS FOR ANISOTROPIC BROWNIAN MOTIONS ON MANIFOLDS

ERLEND GRONG AND STEFAN SOMMER

ABSTRACT. Brownian motion on manifolds with non-trivial diffusion coefficient can be constructed by stochastic development of Euclidean Brownian motions using the fiber bundle of linear frames. We provide a comprehensive study of paths for such processes that are most probable in the sense of Onsager-Machlup, however with path probability measured on the driving Euclidean processes. We obtain both a full characterization of the resulting family of most probable paths, reduced equation systems for the path dynamics where the effect of curvature is directly identifiable, and explicit equations in special cases, including constant curvature surfaces where the coupling between curvature and covariance can be explicitly identified in the dynamics. We show how the resulting systems can be integrated numerically and use this to provide examples of most probable paths on different geometries and new algorithms for estimation of mean and infinitesimal covariance.

1. INTRODUCTION

The Eells-Elworthy-Malliavin [9] construction of Brownian motion applies stochastic development to map Euclidean Brownian motions to Riemannian manifolds. The construction uses a Stratonovich SDE in the orthonormal frame bundle to generate the manifold valued processes. A more general class of processes can be constructed by relaxing the requirement of the SDE to start with an orthonormal frame. This corresponds to choosing a diffusion coefficient with non-trivial covariance between the infinitesimal steps of the process. Such processes have been studied in geometric statistics where they, for example, are used to generate probability distributions on manifolds that can be interpreted as normal distributions [14, 18]. These distributions and the corresponding generating processes are termed anisotropic due to their directionally dependent diffusion, and the probability of observing a given point on the manifold is influenced by this anisotropy which weighs the probability of paths from the starting point to the data.

The most probable paths for a Brownian motion from its starting point to a fixed end point can be described as extremal values of the Onsager-Machlup functional [4]. This notion is generalized to the anisotropic case in [18] by measuring the path probability on the driving process, i.e. the Euclidean Brownian motion that is mapped by stochastic development to the manifold. The resulting family of paths are geodesics for a sub-Riemannian structure on the frame bundle [16].

2010 *Mathematics Subject Classification.* 62R30, 60D05, 53C17.

Key words and phrases. Statistics on Riemannian manifolds, diffusion mean, anisotropic Brownian motion, most probable paths.

The first author is supported by the grant GeoProCo from the Trond Mohn Foundation - Grant TMS2021STG02 (GeoProCo). The second author is supported by the Villum Foundation grant 00022924, and the Novo Nordisk Foundation grant NNF18OC0052000.

In this paper, we give an in-depth study of the family of most probable paths. We fully characterize the family and show that the family is a subset of normal sub-Riemannian geodesics. We derive a reduced system governing the dynamics of the family and make the influence of curvature on the dynamics explicit. We link this to qualitative aspects of the family, particularly showing how the paths tend to directions of high-variance with positive curvature, and low-variance with negative curvature. We furthermore derive new algorithms for mean and infinitesimal covariance estimation using the paths, and show how efficient optimization can be obtained using both properties of the systems - particularly equivariance to scaling of the covariance - and using automatic differentiation as opposed to direct evaluation of adjoint equations.

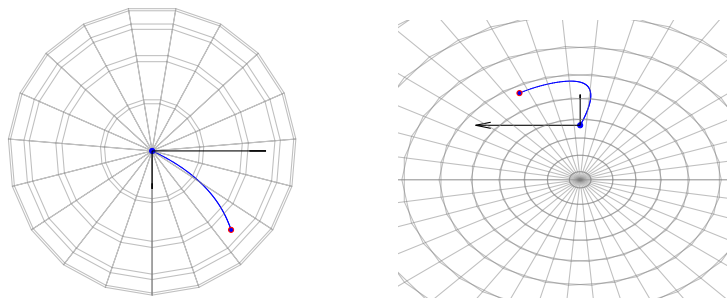


FIGURE 1. Examples of most probable paths on the sphere S^2 (left, view from a pole) and the hyperbolic space H^2 (right). The corresponding frames encoding the diffusion covariance is shown above the starting points (black lines, longer implies higher covariance). Note that the most probable paths tend to the large-covariance direction with positive curvature and to the low-covariance direction with negative curvature.

1.1. Background. Most probable paths for anisotropic diffusion processes were defined in [18] where the Onsager-Machlup [4] functional was used to characterize the path probability from the Euclidean Brownian motion that drives the evolution. The paths were further studied in [15] as projections of sub-Riemannian geodesics on FM with the assumption of normality. The resulting Hamiltonian system provides only sufficient conditions for the paths, and it has not been proved that the normality assumption holds. Results in [15] show experimentally that the anisotropy affects the dynamics of the paths by tending towards the directions of largest variance. In this paper, we prove this hypothesis in the constant positive curvature case, and show that this does not hold - in fact the effect is opposite - with constant negative curvature, see Figure 1. Estimators based on most probable paths have been used in statistical applications in e.g. [14, 17].

1.2. Outline. We start with a brief survey of anisotropic processes on manifolds, their application in geometric statistics, and the relation between geodesic distances, most probable paths, and least-squares constructions exemplified by the Fréchet mean. Section 3 outlines the stochastic process and frame bundle theory used in the paper. In Section 4, we define the sub-Riemannian structures

on $\text{Sym}^+ TM$, FM and OM that encode infinitesimal covariance, we define path probability and quantify the effect on estimators when varying the total variance. Section 5 contains the dynamical equations for most probable paths and consequences of the derived system. We study most probable paths in specific examples in Sections 6 and 7. We further discuss numerical implementation of the systems and provide algorithms for estimation of mean and covariance using most probable paths in Section 8.

2. ANISOTROPIC DISTRIBUTIONS, GEOMETRIC STATISTICS, AND MOST PROBABLE PATHS

We here give a short survey of the relation between mean estimation, infinitesimal covariance, and most probable paths in geometric statistics. Particularly, this leads to most probable paths as extremizers for an objective function that generalize the Fréchet variance. We get estimators for diffusion means in the presence of non-trivial covariance. These estimators depend on the covariance-weighted length of the most probable paths.

2.1. Mean values on Riemannian manifolds. Among the most fundamental constructions in geometric statistics, the statistical analysis of manifold valued data [11], is the Fréchet mean [3], defined as the set of minimizers of the expected square distance to a random variable X on a Riemannian manifold M with metric g and distance d_g :

$$(2.1) \quad E(X) = \underset{x \in M}{\operatorname{argmin}} \mathbb{E}[d_g(X, x)^2] .$$

Unlike the Euclidean mean which can be defined in multiple equivalent ways, Riemannian manifolds have several non-equivalent notions of mean values. The diffusion mean [5, 6] is based on the characterization of the Euclidean mean value as the most likely center point of normal distributions. Distributions generated by Riemannian Brownian motions can be seen as manifold generalizations of Euclidean normal distributions. This results in the diffusion mean set

$$(2.2) \quad E_t(X) = \underset{x \in M}{\operatorname{argmin}} \mathbb{E}[-\ln p_t(X; x)]$$

where $p_t(\cdot; x)$ is the density of a Brownian motion started at $x \in M$ and evaluated at time $t > 0$. Because $\lim_{t \rightarrow 0} -2t \ln p_t(y; x) = d_g(y; x)^2$, diffusion means are linked to the Fréchet mean in the $t \rightarrow 0$ limit.

2.2. Data anisotropy. The diffusion mean (2.2) gives rise the question of what happens if the manifold normal distributions that are fitted to data by maximum likelihood in (2.2) have non-trivial covariance. This case is not covered by distributions generated by Brownian motions that by construction are isotropic since Brownian motions diffuse equally in all directions. To treat this question, [14, 18] defined anisotropic normal distributions on manifolds using Brownian-like processes, however with directionally dependent diffusion coefficients. We write $p_t(y; x, \Sigma)$ for the density of such a process, where $x, y \in M$, x represents the mean of the distribution and $\Sigma \in \text{Sym}^+ T_x M$ is a symmetric, positive definite linear map from $T_x M$ to itself representing the covariance. We will give the construction of these densities

in Section 3.2. For a random variable X , the diffusion mean and covariance (x, Σ) can now be found simultaneously by minimizing the negative log-likelihood

$$(2.3) \quad E_t(X) = \operatorname{argmin}_{(x, \Sigma) \in \operatorname{Sym}^+ TM} \mathbb{E}[-\ln p_t(X; x, \Sigma)].$$

The diffusion PCA construction [17] continues this idea by employing a maximum likelihood fit of such distributions to give a generalization of principal component analysis (PCA) to manifolds.

As for the link between the (isotropic) diffusion mean and the Fréchet mean, one can study the $t \rightarrow 0$ limit of (2.3). This turns out to have a least-squares formulation similar to (2.1), however with the squared Riemannian distance $d_g(\cdot, x)^2$ replaced by a function $d_\rho(\pi^{-1}(\cdot), (x, \Sigma))^2$ that arises from a sub-Riemannian distance on the bundle of symmetric positive definite endomorphisms of TM or, alternatively, the frame bundle of M :

$$(2.4) \quad \lim_{t \rightarrow 0} -2t \ln p_t(y; x, \Sigma) = d_\rho(\pi^{-1}(y), (x, \Sigma))^2.$$

Here π is the fiber bundle projection. The distance d_ρ was defined [18]. We will revisit the definition in Sections 3 and 4. The limit generalizes the standard Brownian motion small-time limit $\lim_{t \rightarrow 0} -2t \ln p_t(y; x) = d_g(y, x)^2$. One can therefore approximate the objective $-\ln p_t(X; x, \Sigma)$ in (2.3) with $\frac{1}{2}d_\rho(\pi^{-1}(X), (x, \Sigma))^2$.

Paths realizing $d_\rho(\pi^{-1}(y), (x, \Sigma))^2$ are in a certain sense most probable for the anisotropic diffusion processes and thus give the most probable ways of getting from the mean to observed data points. The cost $d_\rho(\pi^{-1}(y), (x, \Sigma))^2$ and paths realizing it thus take a dual role in both approximating the objective of (2.3) for small t and in being most-probable for the diffusion process for any $t > 0$. We use both roles in the forthcoming sections.

2.3. Sample estimators. Let now y_1, \dots, y_n be i.i.d. samples on the manifold M . Following [18], consider the sample estimator

$$(2.5) \quad \operatorname{argmin}_{(x, \Sigma)} \frac{1}{n} \sum_{i=1}^n (-\ln p(y_i; x, \Sigma)),$$

of the diffusion mean (2.3). Again, since the density $p(y_i; x, \Sigma)$ generally is complex to approximate computationally, we can use the small- t limit that suggests the approximation [18],

$$(2.6) \quad \operatorname{argmin}_{(x, \Sigma)} \frac{1}{2n} \sum_{i=1}^n \left(d_\rho(\pi^{-1}(y_i); (x, \Sigma))^2 + \ln \det_g \Sigma \right).$$

Again, most probable paths arise as the paths realizing the objective of the sample estimator.

3. FRAME BUNDLE GEOMETRY AND STOCHASTIC DEVELOPMENT

To establish the geometric foundation for the study of most probable paths, we give a short introduction to some of the intrinsic structures that exists on the frame bundle of a Riemannian manifold and that will be used in the paper. Following this, we discuss the stochastic development procedure and its use in defining semi-martingales on manifolds.

3.1. The frame bundle of a Riemannian manifold. In the discussions below, \mathbb{R}^d will always be the d -dimensional Euclidean space and with the standard basis e_1, \dots, e_d . We refer to [12, 8] for more details.

Let M be a d -dimensional differentiable manifold. For any $x \in M$, consider $\text{GL}(T_x M)$ as the space of all linear isomorphisms $u : \mathbb{R}^d \rightarrow T_x M$. Such a map can be identified with a choice of basis u_1, \dots, u_d of $T_x M$ with $u_j = u(e_j)$. The frame bundle $FM = \text{GL}(TM)$ is the principal bundle

$$\text{GL}(d) \rightarrow FM \xrightarrow{\pi} M, \quad FM_x = \text{GL}(T_x M),$$

where $\text{GL}(d)$ acts on each fiber by composition on the right. Using the action of $\text{GL}(d)$, we can associate a vector field ξ_A for each $A \in \mathfrak{gl}(d)$ by

$$\xi_A|_u = \frac{d}{dt} u \cdot e^{tA}|_{t=0}, \quad A \in \mathfrak{gl}(d).$$

These vector fields span the vertical bundle $\mathcal{V} = \ker \pi_*$ and give the relation

$$[\xi_A, \xi_B] = \xi_{[A, B]}, \quad A, B \in \mathfrak{gl}(n).$$

We also have a tautological \mathbb{R}^d -valued one-form θ on FM given by

$$\theta : w \mapsto u^{-1}(\pi_* w), \quad w \in T_u FM.$$

Notice that the kernel of θ is exactly the vertical bundle \mathcal{V} .

Introduce now a Riemannian metric g on M with Levi-Civita connection ∇ . For every smooth curve $t \mapsto \gamma(t)$, there is a ∇ -parallel frame $u(t) \in FM_{\gamma(t)}$ uniquely determined by its value at an initial point. Let \mathcal{H} be the set of derivatives of such curves. Then

$$(3.1) \quad TFM = \mathcal{H} \oplus \mathcal{V}.$$

The subbundle \mathcal{H} is invariant under the group action, and we can hence define a corresponding principal connection $\omega : TFM \rightarrow \mathfrak{gl}(d)$ given by

$$\mathcal{H} = \ker \omega, \quad \omega(\xi_A) = A.$$

For any vector $v \in T_x M$ and $u \in FM_x$, define $h_u v \in \mathcal{H}_u$ as the unique vector projecting to v . Similarly, for any vector field $V \in \Gamma(TM)$, define $hV|_u = h_u V|_{\pi(u)}$. Finally, for an element $a \in \mathbb{R}^d$, we define H_a as the unique vector field satisfying

$$(3.2) \quad \theta(H_a) = a, \quad \omega(H_a) = 0.$$

In other words, if $a = \sum_{i=1}^d a_i e_i$, then $H_a|_u = \sum_{i=1}^d a_i h_u u_i = \sum_{i=1}^d a_i H_i$ where $H_i = H_{e_i}$.

The above definitions have the following local representation. Choose a local orthonormal basis V_1, \dots, V_d of TM and define a corresponding local trivialization

$$FM \cong M \times \text{GL}(d), \quad u \in FM_x \mapsto (x, (u_{ij})), \quad u_j = \sum_{i=1}^d u_{ij} V_i.$$

If we write $\nabla_{V_i} V_j = \sum_{k=1}^n \Gamma_{ij}^k V_k$ for the Christoffel symbols, then

$$\xi_A = \sum_{i,j,r=1}^d u_{ir} A_{rj} \frac{\partial}{\partial u_{ij}}, \quad hV_k = V_k - \sum_{i,j,r=1}^d u_{rj} \Gamma_{kr}^i \frac{\partial}{\partial u_{ij}}, \quad H_a = \sum_{i,j=1}^d a_j u_{ij} hV_i.$$

Write R for the curvature of the Levi-Civita connection. Using the above formulas, we have the local identities

$$\begin{aligned} [hV_k, hV_l] &= h[V_k, V_l] - \sum_{i,j,r=1}^d u_{ir} \langle u^{-1}R(V_k, V_l)u_j, e_r \rangle \frac{\partial}{\partial u_{ij}}, \\ [\xi_A, hV_l] &= 0. \end{aligned}$$

Define $\underline{R}: FM \rightarrow (\mathbb{R}^{d,*})^{\otimes 3} \otimes \mathbb{R}^d$ as the scalarization of the curvature R , given by

$$\underline{R}(u)(a, b)c = u^{-1}R(u(a), u(b))u(c), \quad u \in FM, a, b, c \in \mathbb{R}^d.$$

We use the previous local identities for the Lie brackets to give global formulas

$$(3.3) \quad [H_a, H_b] = -\xi_{\underline{R}(a,b)} \quad [\xi_A, H_a] = H_{Aa}, \quad a, b \in \mathbb{R}^d, A \in \mathfrak{gl}(d).$$

The corresponding identities for forms are given as

$$(3.4) \quad d\omega + \frac{1}{2}[\omega, \omega] = \Omega, \quad d\theta + [\omega, \theta] = 0,$$

where the curvature form Ω vanish on \mathcal{V} and satisfies $\Omega(H_a, H_b)|_u = \underline{R}(u)(a, b)$.

If we restrict ourselves to the orthonormal frame bundle $OM \subseteq FM$, then orthonormal frames remain orthonormal under parallel transport with respect to the Levi-Civita connection. Hence, the above formalism also makes sense if we only consider orthonormal frames. For this reason, by slight abuse of notation, we will also use the symbols \mathcal{H} , θ and ω for the restriction of these to OM .

3.2. Stochastic processes and development. Let $B_t = (B_t^1, \dots, B_t^d)$ be the standard Brownian motion on \mathbb{R}^d , meaning in particular that B_t is normally distributed as $\mathcal{N}(0, t1_d)$. Throughout this section, we will assume that M is a compact manifold which by [13] will also be sufficient for the solutions of the SDEs below on FM to have infinite lifetime. See Remark 3.4 for the noncompact case.

Let FM be the frame bundle of a d -dimensional Riemannian manifold (M, g) . For a given initial frame $u \in FM$, we define $U_t = U_t(u)$ as the solution of the Stratonovich SDE,

$$(3.5) \quad dU_t = H_{\circ dB_t}|_{U_t} = \sum_{i=1}^d H_i|_{U_t} \circ dB_t^i, \quad U_0 = u.$$

Define $X_t(u) = \pi(U_t(u))$ as its projection to M . Here X_t is the *development* of B_t , and the development can be reversed in the sense that B_t can be found from X_t and the initial condition u . In this case, B_t is denoted *the anti-development* of X_t . The stochastic development (3.5) has a deterministic counterpart in the ODE

$$(3.6) \quad \dot{u}(t) = H_{v(t)}|_{u(t)} = \sum_{i=1}^d H_i|_{u(t)} \dot{b}^i(t), \quad u(0) = u.$$

for an absolutely continuous path $b(t)$ in \mathbb{R}^n and with $u(t)$ being a parallel frame along a path $x(t)$.

Let $\text{Sym}^+ TM$ denote positive definite symmetric endomorphisms of TM . Define a map $\Sigma: FM \rightarrow \text{Sym}^+ TM$, $u \mapsto \Sigma_u$ by

$$\langle u^{-1}w_1, u^{-1}w_2 \rangle = \langle \Sigma_u^{-1}w_1, w_2 \rangle_g, \quad u \in FM_x, w_1, w_2 \in T_x M.$$

We observe that Σ_u is always invertible and symmetric, and equals the identity on $T_x M$ if u is orthonormal. Furthermore, if $q \in O(d)$, then $\Sigma_{u \cdot q} = \Sigma_u$. Similarly,

since the Brownian motion is rotationally invariant, we can identify $X_t(u \cdot q)$ with $X_t(u)$ for $q \in O(d)$ and write $X_t(u) = X_t(\Sigma_u)$.

Next, let $\text{Sym}^+ \mathbb{R}^d$ consist of symmetric, positive definite $d \times d$ -matrices. We define a map $S : FM \rightarrow \text{Sym}^+ \mathbb{R}^d$, $u \mapsto S_u$ by

$$\langle S_u^2 a, b \rangle = \langle u(a), u(b) \rangle_g, \quad a, b \in \mathbb{R}^d.$$

We observe that $u^{-1} \Sigma_u u = S_u^2$. Furthermore, since $\langle u(t)a, u(t)b \rangle_g$ is constant in any parallel frame

$$(3.7) \quad H_a S = 0, \quad \text{for any } a \in \mathbb{R}^d.$$

Hence, for some fixed $S \in \text{Sym}^+ \mathbb{R}^d$, if we define

$$F^S M = \{\tilde{u} \in FM : S_{\tilde{u}} = S\},$$

then $U_t(u)$ takes values in $F^{S_u} M$.

There is a diffeomorphism i_S from $F^S M$ to the orthonormal frame bundle $OM \subseteq FM$ given by

$$(3.8) \quad i_S(u) = u \cdot S^{-1}.$$

Let us solve the following SDE on the orthonormal frame bundle. For any $S \in \text{Sym}^+ \mathbb{R}^d$ and $f \in OM$, define $\hat{U}_t = \hat{U}_t(S, f)$ as the solution of

$$(3.9) \quad d\hat{U}_t = H_{SdB_t}|_{\hat{U}_t} = \sum_{i,j=1}^d S_{ij} H_i|_{\hat{U}_t} \circ dB_t^j, \quad \hat{U}_0 = f.$$

Furthermore, we write $\hat{X}_t(S, f) = \pi(\hat{U}_t(S, f))$. Observe that for fixed t , SB_t is distributed as $\mathcal{N}(0, tS^2)$. We also give the following observations.

Proposition 3.1. (a) *For any $u \in FM$, the processes $X_t(u)$ and $\hat{X}_t(S_u, u \cdot S_u^{-1})$ are indistinguishable.*

(b) *For any $\Sigma \in \text{Sym}^+ T_x M$, $x \in M$, let $f \in OM_x$ be any orthonormal frame, and write $S^2 = f^{-1} \Sigma f$. Then $X_t(\Sigma)$ and $\hat{X}_t(S, f)$ are indistinguishable.*

Proof. The result in (a) follows by observing that $U_t(u) \cdot S_u^{-1}$ solves the equation in (3.9). For (b), let $f \in OM$ be chosen. Let \tilde{u} be any frame with $\Sigma_{\tilde{u}} = \Sigma$ and define $\tilde{f} = \tilde{u} \cdot S_{\tilde{u}}^{-1} = f \cdot q$ for some $q \in O(d)$. If $u = \tilde{u} \cdot q^{-1}$, then

$$\Sigma_{\tilde{u}} = \Sigma_u, \quad S_u = q S_{\tilde{u}} q^{-1},$$

and so $u \cdot S_u^{-1} = \tilde{u} \cdot S_{\tilde{u}}^{-1} \cdot q^{-1} = f$. We furthermore have that $S_u^2 = u^{-1} \Sigma_u u = S_u^{-1} f^{-1} \Sigma_u f S_u$, so $S_u^2 = f^{-1} \Sigma_u f$. Since $X_t(u)$ and $X_t(u \cdot q)$ are indistinguishable, the result follows. \square

Definition 3.2 ([14]). *Let (M, g) is a Riemannian manifold and let $\Sigma \in \text{Sym}^+ T_x M$, $x \in M$ be arbitrary. We consider the normal distribution $\mathcal{N}(x, \Sigma)$ on M as the distribution of $X_1(\Sigma)$. The density of $X_t(\Sigma)$ with respect to the Riemannian volume measure is $p_t(\cdot; x, \Sigma)$, and we write $p(\cdot; x, \Sigma) = p_1(\cdot; x, \Sigma)$ for the density of the normal distribution.*

Remark 3.3. (a) As a consequence of Proposition 3.1, no generality is lost by the choice of $t = 1$ in the definition of $\mathcal{N}(x, \Sigma)$ since $X_t(\Sigma) = X_1(t\Sigma)$.

(b) If f is chosen to be an eigenframe of Σ in Proposition 3.1 (b), then $S = \Lambda = \text{diag}\{\lambda_1, \dots, \lambda_d\}$ is a diagonal matrix.

Remark 3.4. If M is non-compact, the processes $X_t(\Sigma)$ and $\hat{X}_t(S, f)$ may only be defined up to an exploding time, but this does not change anything about our above conclusions.

4. SUB-RIEMANNIAN DISTANCE AND MOST PROBABLE PATHS

4.1. Sub-Riemannian structure on symmetric endomorphisms. We now define the sub-Riemannian distance d_ρ that was used in Section 2.2 and that enter in the Onsager-Machlup functional for the most probable paths. Further details of sub-Riemannian structures is outlined in Appendix A. We consider the fiber bundle $\pi : \text{Sym}^+ TM \rightarrow M$. Just as in (3.1), we have a decomposition $T \text{Sym}^+ TM = E \oplus \ker \pi_*$, where E is the derivatives of all curves $\Sigma(t)$ that are parallel along their projection $\pi(\Sigma(t)) = \gamma(t)$. We then define a sub-Riemannian metric ρ on E by

$$\|\dot{\Sigma}(t)\|_\rho^2 = \langle \dot{\Sigma}(t), \dot{\Sigma}(t) \rangle_\rho = \langle \tilde{\Sigma}(t)^{-1} \dot{\gamma}(t), \dot{\gamma}(t) \rangle_g,$$

where $\Sigma(t)$ is any curve tangent to E . Denote the corresponding sub-Riemannian distance by d_ρ .

Let $\Sigma \in \text{Sym}^+ T_x M$ be a fixed element for $x \in M$. For any curve $\gamma : [0, T] \rightarrow M$ with $\gamma(0) = x$, introduce notation $//_t : T_x M \rightarrow T_{\gamma(t)} M$ for the parallel transport along the curve. We define $L^\Sigma(\gamma) = L^\rho(\Sigma(\cdot))$ as the length of the curve

$$(4.1) \quad \Sigma(t) = \Sigma //_t = //_t \Sigma //_t^{-1},$$

with respect to ρ . Then for any $y \in M$,

$$d_\rho(\pi^{-1}(y); (x, \Sigma)) = \inf_{\gamma(0)=x, \gamma(T)=y} L^\Sigma(\gamma).$$

This equation defines the map d_ρ as used in Section 2.

4.2. Alternative description. The sub-Riemannian length $L^\rho(t)(\Sigma(\cdot))$ can also be realized in the following two alternative ways. Let $\Sigma(t)$ be a curve in $\text{Sym}^+ TM$ that is parallel along its projection $\gamma(t)$ with $\Sigma(0) = \Sigma^x \in \text{Sym}^+ T_x M$. Let $u^x \in FM$ be any frame with $\Sigma_{u^x} = \Sigma^x$ and define $u(t)$ by parallel transport along $\gamma(t)$. It then follows that $\Sigma_{u(t)} = \Sigma(t)$ for all t . It also follows that $u(t)$ is tangent to the bundle \mathcal{H} in Section 3. We can then define a sub-Riemannian metric $\tilde{\rho}$ on \mathcal{H} by

$$\begin{aligned} \|\dot{\Sigma}(t)\|_\rho^2 &= \langle \Sigma(t)^{-1} \dot{\gamma}(t), \dot{\gamma}(t) \rangle_g \\ &= \langle u(t)^{-1} \dot{\gamma}(t), u(t)^{-1} \dot{\gamma}(t) \rangle = \langle \theta(\dot{u}(t)), \theta(\dot{u}(t)) \rangle =: \|\dot{u}(t)\|_{\tilde{\rho}}^2. \end{aligned}$$

It follows that $L^\rho(\Sigma(\cdot)) = L^{\tilde{\rho}}(u(\cdot))$. Observe that $(FM, \mathcal{H}, \tilde{\rho})$ has a global orthonormal basis H_1, \dots, H_d , in contrast to $\text{Sym}^+ TM$.

We can also consider the problem on the orthonormal frame bundle OM . Let $f^x \in OM_x$ be any initial frame and define $S^2 = (f^x)^{-1} \Sigma^x f^x$. If we define $f(t)$ by parallel transport, then $S^2 = f(t)^{-1} \Sigma(t) f(t)$ for any t . We introduce a corresponding sub-Riemannian metric ρ_S on \mathcal{H} , now considered as the bundle of derivatives of parallel orthogonal frames. We define it by

$$\|\dot{\Sigma}(t)\|_\rho^2 = \langle S^{-2} f(t)^{-1} \dot{\gamma}(t), f^{-1} \dot{\gamma}(t) \rangle_g =: \|\dot{f}(t)\|_{\rho_S}^2.$$

In other words, $(OM, \mathcal{H}, \rho_S)$ has global orthonormal basis $H_{Se_1}, \dots, H_{Se_d}$. By the above equality, the lengths $L^\rho(\Sigma(\cdot))$ and $L^{\rho_S}(f(\cdot))$ coincides.

In what follows, we will often state our results using the formulation on $\text{Sym}^+ TM$, as this does not require any choice of initial frame. However, we will usually present

our proofs on OM , as this reduces the problem to a space of minimal dimension and provides access to a global basis for the horizontal subbundle.

4.3. Path probability. Consider the stochastic process $X_t(\Sigma)$ defined in Section 3.2. The process is generated by a Euclidean Brownian motion B_t through the SDE in (3.5). The Onsager-Machlup functional measures the probability that realizations of B_t sojourns around smooth paths in the sense of staying in $\epsilon > 0$ diameter cylinders. More precisely, for paths $b \in C^1([0, T], \mathbb{R}^d)$, define

$$(4.2) \quad \mu_\epsilon(b) = P(\|B_t - b(t)\| < \epsilon \ \forall t \in [0, T]).$$

It can now be shown [4] that $\log \mu_\epsilon(b)$ tends to $c_1 + c_2/\epsilon^2 - \frac{1}{2} \int_0^T \|\dot{b}(t)\|^2 dt$ for constants c_1, c_2 as $\epsilon \rightarrow 0$. One here recognizes the usual Euclidean energy of b . Paths between two points maximizing this Onsager-Machlup functional are termed most probable. Here, we look at paths $b(t)$ such that the corresponding development (3.6) of b starts at $u \in FM$ with $\Sigma_u = \Sigma$ and ends with the projection $\gamma(t) = \pi(u(t))$ to M satisfying $\gamma(T) = y$. Then $\gamma(t)$ is termed most probable for $Y_t(\Sigma)$ given by (3.5) if it realizes

$$(4.3) \quad \max_{\Sigma_{u(0)} = \Sigma, \gamma(T) = y} -\log \mu_\epsilon(b) = \min_{\Sigma_{u(0)} = \Sigma, \gamma(T) = y} \frac{1}{2} \int_0^T \|\dot{b}(t)\|^2 dt = d_\rho(\pi^{-1}(y), \Sigma)^2$$

for $y \in M$. Extremal paths for $L^\rho(\Sigma(\cdot))$ thus have a probabilistic characterization as being *most probable* with respect to $X_t(\Sigma)$.

4.4. Covariance scaling and optimal estimators. Let $\Sigma(t) \in \text{Sym}^+ T_{\gamma(t)} M$ be a parallel along its projection $\gamma(t)$. Then $C\Sigma(t)$ is still parallel along $\gamma(t)$ for any positive constant $C > 0$, so we have $L^\rho(C\Sigma(\cdot)) = C^{-1/2} L^\rho(\Sigma(\cdot))$. Also $\pi^{-1}(y)$ is invariant under multiplication of positive scalars. Hence, if we write $\Sigma = C\Sigma'$ with $\det \Sigma' = 1$, then for samples y_1, \dots, y_n ,

$$\frac{1}{2n} \sum_{i=1}^n \left(d_\rho(\pi^{-1}(y_i), \Sigma)^2 + \ln \det \Sigma \right) = \frac{1}{2} \ln C + \frac{1}{2nC} \sum_{i=1}^n d_\rho(\pi^{-1}(y_i), \Sigma')^2$$

We then see that the optimal choice for C is

$$(4.4) \quad C = \frac{1}{n} \sum_{i=1}^n d(\pi^{-1}(y_i), \Sigma')^2.$$

Furthermore,

$$\begin{aligned} \Sigma' &= \underset{\substack{\tilde{\Sigma} \in \text{Sym}^+ TM \\ \det \tilde{\Sigma} = 1}}{\text{argmin}} \left(\ln C + \frac{1}{nC} \sum_{i=1}^n d_\rho(\pi^{-1}(y_i), \tilde{\Sigma})^2 \right) \Big|_{C = \frac{1}{n} \sum_{i=1}^n d(\pi^{-1}(y_i), \tilde{\Sigma})^2} \\ &= \underset{\substack{\tilde{\Sigma} \in \text{Sym}^+ TM \\ \det \tilde{\Sigma} = 1}}{\text{argmin}} \left(\ln \left(\sum_{i=1}^n d_\rho(\pi^{-1}(y_i), \tilde{\Sigma})^2 \right) - \ln n + 1 \right), \end{aligned}$$

which implies that

$$(4.5) \quad \Sigma' = \underset{\substack{\tilde{\Sigma} \in \text{Sym}^+ TM \\ \det \tilde{\Sigma} = 1}}{\text{argmin}} \sum_{i=1}^n d_\rho(\pi^{-1}(y_i), \tilde{\Sigma})^2.$$

The result is the following reduced optimization problem for sample estimators. The separate optimization for Σ' and total variance C can ease numerical optimization, see Section 8.

Proposition 4.1. *The sample estimate (2.6) can be found by solving (4.5) to obtain optimal $\Sigma' \in \text{Sym}^+ TM$, $\det \tilde{\Sigma} = 1$ followed by setting $\Sigma = C\Sigma'$ with C is given by (4.4).*

5. DYNAMICS

5.1. Equations for most probable paths. We can now state and prove the main theorem of the paper that characterizes the dynamics of most probable paths. In the follow subsections, we describe the most important direct consequences of the theorem. Recall that the covariant derivative along the curve γ is given by $D_t = \nabla_{\dot{\gamma}(t)} = //_{\dot{\gamma}(t)} \frac{d}{dt} //_{\dot{\gamma}(t)}^{-1}$.

Theorem 5.1. *Assume that $\gamma : [0, T] \rightarrow M$ is the most probable curve from x to $y = \gamma(T)$ with respect to the covariance $\Sigma \in \text{Sym}^+ T_x M$. Then up to reparametrization, the curve solves the following equation. If $\Sigma_{//t}$ is as in (4.1), then γ solves the equation*

$$(5.1) \quad \begin{cases} D_t \dot{\gamma}(t) = \Sigma_{//t} R(\chi(t)) \dot{\gamma}(t), \\ D_t \chi(t) = \dot{\gamma}(t) \wedge \Sigma_{//t}^{-1} \dot{\gamma}(t), \\ \chi(T) = 0 \end{cases}$$

Note the explicit role of the Riemannian curvature tensor R in the dynamics for γ . The infinitesimal covariance Σ affects both the γ and χ evolution.

Proof. Recall the notation on the frame bundle introduced in Section 3, and in particular the equations (3.4). Let $\Sigma \in \text{Sym}^+ T_x M$ and $y \in M$ be fixed. Using the realization in Section 4.2, we consider the problem on OM . Let $f^x \in OM_x$ be any orthonormal frame and define $S^2 = (f^x)^{-1} \Sigma f^x$. We then want to find a curve $f(t)$ defined on $[0, T]$ such that $f(t)$ is parallel along its projection $\gamma(t)$ in M , $f(0) = f^x$ and that $f(t)$ is an extremal with respect to the length

$$L^\Sigma(\gamma) = \int_0^T \|S^{-1} f(t)^{-1} \dot{\gamma}(t)\| dt,$$

among all such curves with $\gamma(T) = y$.

Consider the Hilbert manifold $\mathcal{C}(f^x)$ of absolutely continuous \mathcal{H} -horizontal curves $f : [0, T] \rightarrow OM$ with $f(0) = f^x$ and with $\dot{f}(t)$ in L^2 , see Appendix A for details. If $s \mapsto f_s(\cdot)$ is a smooth curve in $\mathcal{C}(f^x)$ then since

$$f_s(0) = f^x, \quad \text{and} \quad \omega(\dot{f}_s(t)) = 0,$$

we know that

$$\partial_s f_s(0) = 0, \quad \partial_t \omega(\partial_s f_s) = d\omega(\dot{f}_s, \partial_s f_s) = \Omega(\dot{f}_s, \partial_s f_s) = \underline{R}(f_s)(\theta(\dot{f}_s), \theta(\partial_s f_s)).$$

Any tangent vector of $\mathcal{C}(f^x)$ at $t \mapsto f(t)$ can be considered as a vector field $W(t)$ along $f(t)$, such that

$$(5.2) \quad W(t) = \left(H_{w(t)} + \xi_{\int_0^t \underline{R}(f(\tau))(\theta(\dot{f}(\tau)), w(\tau)) d\tau} \right) \Big|_{f(t)}, \quad w(0) = 0,$$

for some $w \in L^2([0, T], \mathbb{R}^d)$ with $w(0) = 0$.

Consider now the endpoint map $\Pi : \mathcal{C}(f^x) \rightarrow M$ given by $f(\cdot) \mapsto \pi(f(T))$. We then see that the differential at $f(\cdot)$ for a vector field W as in (5.2) is

$$\Pi_* W = \sum_{i=1}^d w_i(T) f_i(T).$$

It follows that every point $y \in M$ is a regular value of Π , and so the preimage $\mathcal{C}(f^x, \pi^{-1}(y)) = \Pi^{-1}(y)$ of curves from f^x to $\pi^{-1}(y)$ is a Hilbert manifold as well from the inverse function theorem. Tangent vectors are then vector fields W as in (5.2) with the extra restriction that $w(T) = 0$.

To complete our computation for the first order condition for optimality, we will introduce some notation. We identify elements in $\wedge^2 \mathbb{R}^d$ with elements in $\mathfrak{so}(d)$ such that for $a, b, c \in \mathbb{R}^d$, the two-vector $a \wedge b$ is identified with the map in $\mathfrak{so}(d)$ given by

$$(a \wedge b)c = \langle a, c \rangle b - \langle b, c \rangle a.$$

Conversely, a matrix $A = (A_{ij})$ is identified with the two-vector

$$\sum_{i < j} A_{ij} e_j \wedge e_i = \frac{1}{2} \sum_{i,j=1}^d A_{ij} e_j \wedge e_i.$$

Define an inner product on $\mathfrak{so}(d)$ by

$$(5.3) \quad \langle A, B \rangle = -\frac{1}{2} \operatorname{tr} AB, \quad A, B \in \mathfrak{so}(d).$$

We note the relation

$$\langle A, a \wedge b \rangle = \langle Aa, b \rangle.$$

Furthermore, if f is any orthonormal frame, then we will have

$$\langle \underline{R}(f)(a, b), A \rangle = \langle \underline{R}(f)(A), a \wedge b \rangle.$$

We look for critical points of the energy functional

$$E(f(\cdot)) = \frac{1}{2} \int_0^T \left| S^{-1} \theta(\dot{f}(t)) \right|^2 dt,$$

on the manifold $\mathcal{C}(f^\mu, \pi^{-1}(y))$. Let $s \mapsto f_s$ be any smooth curve in $\mathcal{C}(f^\mu, \pi^{-1}(y))$ with $f_0(t) = f(t)$ and $\partial_s f|_{s=0}(t) = W(t)$. Write

$$\theta(W(t)) = w(t), \quad \theta(\dot{f}(t)) = v(t),$$

and recall that then

$$w(0) = w(T) = 0, \quad \omega(W(t)) = \int_0^t \underline{R}(f(\tau))(v(\tau), w(\tau)) d\tau.$$

If $f(t)$ is a local minimum of the energy, then

$$\begin{aligned} 0 &= \partial_s E(f_s)|_{s=0} = \int_0^T \langle S^{-2} \theta(\dot{f}_s(t)), \partial_s \theta(\dot{f}_s(t)) \rangle dt|_{s=0} \\ &= \int_0^T \left\langle S^{-2} \theta(\dot{f}_s(t)), \partial_t \theta(\partial_s f_s(t)) \right\rangle dt|_{s=0} + \int_0^T \langle S^{-2} \theta(\dot{f}_s(t)), d\theta(\partial_s f_s, \dot{f}_s(t)) \rangle dt|_{s=0} \\ &= \int_0^T \langle S^{-2} v(t), \dot{w}(t) \rangle dt - \int_0^T \langle S^{-2} v(t), \omega(W(t)) v(t) \rangle dt \end{aligned}$$

$$= - \int_0^T \langle S^{-2} \dot{v}(t), w(t) \rangle dt - \int_0^T \left\langle v(t) \wedge S^{-2} v(t), \int_0^t \underline{R}(f(\tau))(v(\tau), w(\tau)) d\tau \right\rangle dt$$

Defining $A(t) = \int_0^t v(\tau) \wedge S^{-2} v(\tau) d\tau$ as a curve in $\mathfrak{so}(d)$, and using integration by parts

$$\begin{aligned} 0 &= - \int_0^T \langle S^{-2} \dot{v}(t), w(t) \rangle dt - \left\langle A(T), \int_0^T \underline{R}(f(t))(v(t), w(t)) dt \right\rangle dt \\ &\quad + \int_0^T \langle A(t), \underline{R}(f(t))(v(t), w(t)) \rangle dt \\ &= \int_0^T \langle -S^{-2} \dot{v}(t) + \underline{R}(f(t))(A(t) - A(T))v(t), w(t) \rangle dt. \end{aligned}$$

It follows that

$$\dot{v}(t) = S^2 \underline{R}(f(t))(A(t) - A(T))v(t).$$

The result follows by defining $\chi(t) = \frac{1}{2} \sum_{i,j=1}^d (A_{ij}(t) - A_{ij}(T)) f_j(t) \wedge f_i(t)$. \square

Remark 5.2. The solutions in Theorem 5.1 are the ones parametrizes such that $|\Sigma_{//t}^{-1/2} \dot{\gamma}(t)| = c$ is a first integral. We can see this directly from

$$\frac{1}{2} \frac{d}{dt} |\Sigma_{//t}^{-1/2} \dot{\gamma}(t)|^2 = \langle \Sigma_{//t}^{-1} D_t \dot{\gamma}(t), \dot{\gamma}(t) \rangle = - \langle R(\chi(t)) \dot{\gamma}(t), \dot{\gamma}(t) \rangle = 0.$$

It follows that $L^\Sigma(\gamma) = cT$.

5.2. Consequences of Theorem 5.1. We look at some immediate consequences of our previous result. We first make a statement about normal geodesics, see Appendix A for definition.

Corollary 5.3. *Consider $\text{Sym}^+ TM$ with the sub-Riemannian metric ρ . Solutions of (5.1) are normal geodesics of ρ . Conversely, normal geodesics of ρ are the solutions of (5.1) with the condition $\chi(T) = 0$ omitted.*

Proof. This results follows from a similar computation as in the proof of Theorem 5.1, but from a Hamiltonian rather than a Lagrangian perspective. We leave the details in Appendix B. \square

Most probable paths were previously studied as normal geodesics without the end-point condition $\chi(T) = 0$ and with the assumption of normality [15]. The corollary makes this assumption unnecessary and strengthens the characterization with the end-point condition. One can consider the condition $\chi(T) = 0$ as ensuring that our endpoint is the optimal point in $\pi^{-1}(y)$. For a simple analogue, one may consider the distance from a point to a line in \mathbb{R}^2 , where the optimal path is a geodesic with the final condition that it must hit the line orthogonally.

5.3. Representation in a parallel frame. We can write the system (5.1) in a parallel frame as follows. This concrete form can be used for numerical integration of the system.

Let $f \in OM_x$ be an arbitrary initial frame and define $f(t)$ by parallel transport. Write $f(t)^{-1} \Sigma f(t) = S^2$. Let (S^{ij}) be the inverse of S . Write

$$(5.4) \quad \begin{aligned} v(t) &= (v_1(t), \dots, v_d(t))^{\dagger} = f(t)^{-1} \dot{\gamma}(t) \\ R_{ijkl}(t) &= \langle f_l(t), R(f_i(t), f_j(t)) f_k(t) \rangle_g. \end{aligned}$$

Finally, consider a matrix $(\chi_{ij}(t))$ in $\mathfrak{so}(d)$ such that $\chi(t) = \frac{1}{2} \sum_{i,j=1}^d \chi_{ij}(t) f_j(t) \wedge f_i(t)$. The above equations take the form

$$(5.5) \quad \begin{cases} \dot{v}_r(t) = \frac{1}{2} \sum_{i,j,k,l=1}^d S_{rs} S_{sl} R_{jikl}(t) \chi_{ij}(t) v_k(t), \\ \dot{\chi}_{ij}(t) = \sum_{k=1}^d (v_j(t) S^{ik} - v_i(t) S^{jk}) S^{kl} v_l(t), \\ \chi_{ij}(T) = 0. \end{cases}$$

The dependence on the parallel frame $f(t)$ are in the coefficients $R_{jikl}(t)$, unless $\nabla R = 0$, in which these coefficients are constant. If we choose f as eigenframe, then $S = \Lambda = \text{diag}\{\lambda_1, \dots, \lambda_d\}$ is a diagonal matrix, and the equations in (5.5) reduce to

$$\dot{v}_l(t) = \frac{\lambda_l^2}{2} \sum_{i,j,k=1}^d R_{jikl}(t) \chi_{ij}(t) v_k(t), \quad \dot{\chi}_{ij}(t) = \frac{\lambda_j^2 - \lambda_i^2}{\lambda_i^2 \lambda_j^2} v_i(t) v_j(t).$$

6. MOST PROBABLE PATHS ON SURFACES

6.1. Equations for most probable paths. We now explore the particular equations for the case when $d = 2$. For $y \in M$, let $\kappa(y)$ be the Gaussian curvature of M at $y \in M$.

Corollary 6.1. *For a given $\Sigma \in \text{Sym}^+ T_x M$, $x \in M$, let $\lambda_1 \geq \lambda_2 > 0$ be its eigenvalues. For a curve $\gamma : [0, T] \rightarrow M$ starting at x , define $f_1(t)$, $f_2(t)$ as a parallel eigenframe of $\Sigma_{//t}$ along $\gamma(t)$ such that $f_j(t)$ corresponds to λ_j . Then γ is the solution of*

$$\dot{\gamma}(t) = c\lambda_1 \cos \theta(t) f_1(t) + c\lambda_2 \sin \theta(t) f_2(t),$$

with

$$(6.1) \quad \dot{\theta}(t) = c^2 \kappa(\gamma(t)) h(t), \quad \dot{h}(t) = -\frac{\lambda_1^2 - \lambda_2^2}{2} \sin 2\theta(t), \quad h(T) = 0.$$

Proof. We write $c = \|\Sigma_{//t}^{-1} \dot{\gamma}\|_g$ for the first integral and write

$$\dot{\gamma}(t) = c\lambda_1 \cos \theta(t) f_1(t) + c\lambda_2 \sin \theta(t) f_2(t).$$

Write $\chi(t) = \frac{c^2}{\lambda_1 \lambda_2} h(t) f_2(t) \wedge f_1(t)$. The equations in (5.5) then becomes (6.1). \square

6.2. Example: Constant curvature surfaces. For any $-\frac{\pi}{2} \leq y \leq \frac{\pi}{2}$, $0 \leq k \leq 1$, we define the elliptic integral of first kind by

$$F(y, k) = \int_0^y \frac{ds}{\sqrt{1 - k^2 \sin^2 s}},$$

with the complete version $K(k) = F(\frac{\pi}{2}, k)$. Correspondingly, we define the Jacobi elliptic sine function $\text{sn}(y, k)$ by $\text{sn}(F(y, k), k) = \sin y$. We define the corresponding delta amplitude as $\text{dn}(y, k) = \sqrt{1 - k^2 \text{sn}(y, k)^2}$.

The following result for constant curvature surfaces has the qualitative consequence of most probable paths tending towards the direction of highest eigenvalue λ_1 with positive curvature, and towards the direction of lowest eigenvalue λ_2 with negative curvature. It was hypothesized in [15] that the behaviour would be as in

the positive curvature case. The result thus answer affirmative to this hypothesis, however only in the positive curvature case. See also Figure 1.

Theorem 6.2. *Let (M, g) be a two-dimensional manifold of constant Gaussian curvature κ . Let $\Sigma \in \text{Sym}^+ T_x M$ be a chosen element with eigenvalues $\lambda_1 \geq \lambda_2 > 0$ and with corresponding eigenvectors f_1^x, f_2^x . Let γ be a most probable path with respect to Σ , normalized by $\|\Sigma_{//t}^{-1/2} \dot{\gamma}(t)\|_g = 1$ and with $f_j(t) = //_t f_j^x$. If $\kappa > 0$, the most probable paths will be on the form*

$$\dot{\gamma}(t) = \pm \lambda_1 \text{dn}(K(k) + \alpha(T - t), k) f_1(t) + \lambda_2 k \text{sn}(K(k) + \alpha(T - t), k) f_2(t).$$

Conversely, if $\kappa < 0$, most probable paths will take the form

$$\dot{\gamma}(t) = \lambda_1 k \text{sn}(K(k) + \alpha(T - t), k) f_1(t) \pm \lambda_2 \text{dn}(K(k) + \alpha(T - t), k) f_2(t).$$

Proof. For $\alpha > 0$ and a given initial value $-\pi < \psi_0 < \pi$, consider $\psi(t) = \psi(t; \psi_0, \alpha)$ as the solution of the non-linear pendulum equation

$$\ddot{\psi}(t) + \alpha^2 \sin \psi(t) = 0, \quad \psi(0) = \psi_0, \quad \dot{\psi}(0) = 0.$$

It is classical that the solution of this equation is

$$\psi(t) = 2 \sin^{-1}(k \text{sn}(K(k) - \alpha t, k)), \quad k = \sin \frac{\psi_0}{2},$$

with period $2\tau = \frac{4K(k)}{\alpha}$. We note that $\dot{\psi}(t) = 0$ if and only if $t = n\tau$ for some integer n .

Assume now that (M, g) is a two-dimensional manifold of constant Gaussian curvature κ . We can then rewrite the equations (6.1) as

$$(6.2) \quad 2\ddot{\theta} + (\lambda_1^2 - \lambda_2^2)\kappa \sin 2\theta = 0, \quad \dot{\theta}(T) = 0.$$

First consider $\kappa = \frac{1}{r^2} > 0$. Define $\alpha^2 = (\lambda_1^2 - \lambda_2^2)\kappa$. Then $2\theta(t)$ is the solution of the non-linear pendulum equation. By possibly replacing $f_1(t)$ with $-f_1(t)$, we may assume that $-\frac{\pi}{2} \leq \theta(0) \leq \frac{\pi}{2}$. If $\theta(0) = \pm \frac{\pi}{2}$, then the only solution is a constant solution. For $-\frac{\pi}{2} < \theta(0) < \frac{\pi}{2}$, it follows that $\theta(t) \in (-\frac{\pi}{2}, \frac{\pi}{2})$ for all time. As a consequence, we must have that for some $\psi_0 \in (-\pi, \pi)$,

$$\theta(t) = \frac{1}{2} \psi(t - T; \psi_0, \alpha).$$

Note that $\theta(t)$ has period

$$2\tau = \frac{4K(k)}{\alpha} = \frac{4K(\sin^{-1} \frac{\psi_0}{2})}{(\lambda_1^2 - \lambda_2^2)\kappa}.$$

In summary, most probable paths will be on the form

$$(6.3) \quad \begin{aligned} \dot{\gamma}(t) &= v_1(t)f_1(t) + v_2(t)f_2(t) = \pm \lambda_1 \cos(\theta(t))f_1(t) + \lambda_2 \sin(\theta(t))f_2(t) \\ &= \pm \lambda_1 \text{dn}(K(k) + \alpha(T - t), k) f_1(t) + \lambda_2 k \text{sn}(K(k) + \alpha(T - t), k) f_2(t) \end{aligned}$$

If $\kappa = -\frac{1}{r^2} < 0$, then $\pi - 2\theta$ solves the pendulum equation with $\alpha = \sqrt{(\lambda_1^2 - \lambda_2^2)|\kappa|}$. We will then have similar results, with the difference that we now have oscillations in the direction of $f_2(t)$ rather than $f_1(t)$. In other words,

$$\begin{aligned} \dot{\gamma}(t) &= v_1(t)f_1(t) + v_2(t)f_2(t) \\ &= \lambda_1 k \text{sn}(K(k) + \alpha(T - t), k) f_1(t) \pm \lambda_2 \text{dn}(K(k) + \alpha(T - t), k) f_2(t). \quad \square \end{aligned}$$

We can solve (6.3) in $\text{SO}(3)$ if M is identified as a subset of the sphere with radius $r = \kappa^{-1/2}$, centered at the origin. Let $q(t) \in \text{SO}(3)$ be the solution of

$$q(t)^{-1}\dot{q}(t) = \frac{1}{r} \begin{pmatrix} 0 & 0 & v_1(t) \\ 0 & 0 & v_2(t) \\ -v_1(t) & -v_2(t) & 0 \end{pmatrix}, \quad q(0) = 1_3.$$

If we consider $f_1(0)$, $f_2(0)$ and the initial point x as elements in \mathbb{R}^3 , the solution is given by

$$\gamma(t) = \begin{pmatrix} f_1(0) & f_2(0) & \frac{1}{r}x \end{pmatrix} q(t) \begin{pmatrix} 0 \\ 0 \\ r \end{pmatrix}.$$

Examples are visualized in the Figures 2, 3, 4 numerical integration in $\text{SO}(3)$. These are completed in MATLAB using a modification of the DiffMan package [2].

Similarly, in the $\kappa < 0$ case, we can consider M as a subset of $\mathbb{R}^{2,1}$ with $\langle a, a \rangle = -r^2$ and solve (6.3) in $\text{SO}(2, 1)$ with such that

$$q(t)^{-1}\dot{q}(t) = \frac{1}{r} \begin{pmatrix} 0 & 0 & v_1(t) \\ 0 & 0 & v_2(t) \\ v_1(t) & v_2(t) & 0 \end{pmatrix}, \quad \gamma(t) = \begin{pmatrix} f_1(0) & f_2(0) & \frac{1}{r}x \end{pmatrix} q(t) \begin{pmatrix} 0 \\ 0 \\ \frac{1}{r} \end{pmatrix}.$$

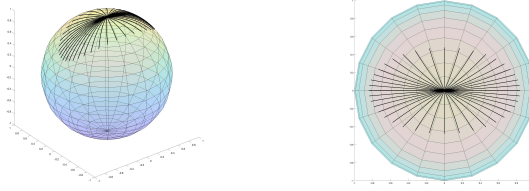


FIGURE 2. The figures above show examples of most probable paths on the unit sphere starting at the north pole with $\lambda_1 = 2$ and $\lambda_2 = 1$. The two figures show examples of most probable paths with $T = 1/2$ seen from the side and above.

7. LOCALLY SYMMETRIC AND SYMMETRIC SPACES

Let now (M, g) be a locally symmetric space, i.e. a space where the curvature satisfies $\nabla R = 0$. We consider a given mean $x \in M$ and covariance $\Sigma \in \text{Sym}^+ T_x M$. Let f^x be an orthonormal eigenframe of Σ with corresponding eigenvalues given by the diagonal matrix $\Lambda^2 = \text{diag}\{\lambda_1^2, \dots, \lambda_d^2\}$. Let $G \subseteq OM$ be the subset of frames that can be obtained by parallel transport of f^x . Then there is some subgroup $H \subseteq O(d)$ of elements q such that $f^x \cdot q \in G$ and we have a principal bundle structure

$$H \rightarrow G \xrightarrow{\pi} M.$$

We note that $\underline{R} = \underline{R}(f)$ is constant for every $f \in G$, and by the Ambrose-Singer theorem, the image of \underline{R} spans the Lie algebra $\mathfrak{h} \subseteq \mathfrak{so}(d)$ of H . Define a Lie algebra \mathfrak{g} as the vector space $\mathbb{R}^d \times \mathfrak{h} \subseteq \mathbb{R}^d \times \mathfrak{so}(d)$ with Lie brackets

$$[(a, A), (b, B)]_{\mathfrak{g}} = (Ab - Ba, -\underline{R}(a, b) + [A, B]).$$

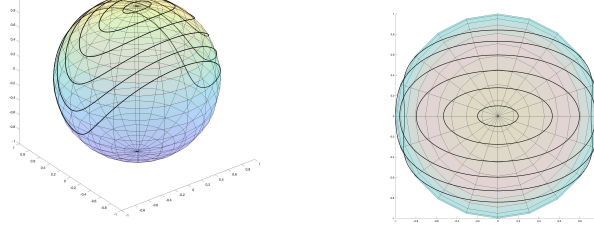


FIGURE 3. For the unit sphere with $\lambda_1 = 2$ and $\lambda_2 = 1$, we have mapped the endpoints of the most probable paths for different values of T .

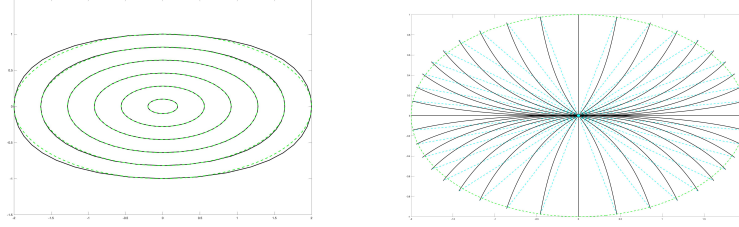


FIGURE 4. Again, we consider the unit sphere with $\lambda_1 = 2$ and $\lambda_2 = 1$, but now in a normal coordinate system centered at the north pole. The first image shows the endpoints compared to ellipses. The second shows most probable paths relative to geodesics.

This is a well-defined Lie algebra since $[A, \underline{R}(a, b)]_{\mathfrak{g}} = \underline{R}(Aa, b) + \underline{R}(a, Ab)$ for any $a, b \in \mathbb{R}^d$ and $A \in \mathfrak{h}$. We will use this Lie group structure to give the following result.

Corollary 7.1. *Let $\gamma : [0, T] \rightarrow M$ be a curve starting at $x \in M$, with $v(t) = (f^x)^{-1} //_{\gamma}^{-1} \dot{\gamma}(t)$. Assume that $\gamma(t)$ is a most probable path. Then there is a curve $B(t)$ in \mathfrak{h} such that*

$$\frac{d}{dt}(\Lambda^{-2}v(t), B(t)) = -[(v(t), 0), (\Lambda^{-2}v(t), B(t))]_{\mathfrak{g}}, \quad B(T) = 0.$$

Proof. In the notation of Section 5.3, if $B(t) = \frac{1}{2} \sum_{i,j=1}^d \chi_{ij}(t) \underline{R}(e_j, e_i)$, then

$$\Lambda^{-2}\dot{v}(t) = B(t)v(t), \quad \dot{B}(t) = \underline{R}(v(t), \Lambda^2v(t)).$$

The result follows. \square

Let us now continue to the case the structure of \mathfrak{g} integrates to a Lie group structure on G such that $M = G/H$ is a symmetric space. Define $\gamma : [0, T] \rightarrow M$ as the most probable path relative to a covariance $\Sigma \in \text{Sym}^+ T_x M$. Let $\Lambda^2 = \text{diag}\{\lambda_1^2, \dots, \lambda_d^2\}$ be the eigenvalues of Σ with an eigenframe f^x . Let $f : [0, T] \rightarrow G$ be the solution of $f(t)^{-1} \cdot \dot{f}(t) = (v(t), 0)$ and $f(0) = f^x$, i.e. the result of parallel

transporting f^x . Define $\Phi(t) = (f^x)^{-1} \cdot f(t)$ and write $v_0 = (f^x)^{-1}\dot{\gamma}(0)$, Notice that

$$\Phi(t)^{-1} \cdot \dot{\Phi}(t) = (v(t), 0).$$

We then have the following result.

Proposition 7.2. *Consider the maps $\text{pr}_{\Lambda^{\pm 2}} : \mathfrak{g} \rightarrow \mathfrak{g}$ given by*

$$\text{pr}_{\Lambda^{\pm 2}}(a, A) = (\Lambda^{\pm 2}a, 0), \quad a \in \mathbb{R}^d, A \in \mathfrak{h}.$$

Then $\Phi(t)$ is a solution of

$$\dot{\Phi}(t) = \Phi(t) \text{pr}_{\Lambda^2} \text{Ad}(\Phi(t)^{-1} \Phi(T)) \text{pr}_{\Lambda^{-2}} \Phi(T) \cdot \dot{\Phi}(T).$$

Proof. We then see that by Corollary 7.1,

$$\frac{d}{dt} \text{Ad}(\Phi(t))(\Lambda^{-2}v(t), B(t)) = (0, 0).$$

Hence, for some constant $(c, C) \in \mathfrak{g}$, we have

$$\text{Ad}(\Phi(t))(\Lambda^{-2}v(t), B(t)) = (c, C).$$

Inserting $t = T$, we have

$$\text{Ad}(\Phi(T))(\Lambda^{-2}v_T, 0) = (c, C).$$

Using that $(v(t), 0) = \Phi(t)^{-1} \cdot \dot{\Phi}(t)$, we have the result. \square

Example 7.3. Consider the special case of $M = S^d$, where $G = \text{SO}(d+1)$. In this case, $\mathfrak{g} = \mathfrak{so}(d+1)$ and if we write

$$\mathfrak{g} = \mathfrak{m} \oplus \mathfrak{h} = \left\{ \bar{A} = \begin{pmatrix} A & a \\ -a^\dagger & 0 \end{pmatrix} : A \in \mathfrak{so}(d), a \in \mathbb{R}^d \right\},$$

where \mathfrak{m} and \mathfrak{h} correspond to respectively the cases when $A = 0$ and $a = 0$. If we define

$$I = \begin{pmatrix} 1_d & 0 \\ 0 & 0 \end{pmatrix}, \quad \bar{\Lambda} = \begin{pmatrix} \Lambda & 0 \\ 0 & 1 \end{pmatrix},$$

we then see that

$$\text{pr}_{\Lambda^{\pm 2}} \bar{A} = \bar{\Lambda}^{\pm 1}(\bar{A} - I\bar{A}I)\bar{\Lambda}^{\pm 1}.$$

The equation we have to solve is then

$$\dot{\Phi}(t) = \Phi(t)\Lambda(\Phi(t)^{-1}\bar{B}\Phi(t) - I\Phi(t)^{-1}\bar{B}\Phi(t)I)\Lambda,$$

with $\bar{B} = \Phi(T)\Lambda^{-1}(\Phi(T) \cdot \dot{\Phi}(T) - I\Phi(T) \cdot \dot{\Phi}(T)I)\bar{\Lambda}^{-1}\Phi(T)^{-1}$.

8. ALGORITHMS

We here describe algorithms for computing mean and covariance on both S^2 and more general cases. On S^2 we obtain a very efficient approximate solution, and on general manifolds using constrained optimization. In addition, we describe strategies for numerically integrating the most probable path dynamical equation, and how to optimize over those using automatic differentiation.

8.1. Mean and covariance on S^2 . We show a particular case for constructing an algorithm for the unit sphere S^2 . Let y_1, \dots, y_n be i.i.d. samples on M . We want to find $\Sigma = C\Sigma'$ that minimize (2.6). We only need to find Σ' and then can determine C by (4.4).

- (1) Using a 2 to 1 surjection, we can see the set $\{\tilde{\Sigma} \in \text{Sym}^+ TS^2 : \det \tilde{\Sigma} = 1\}$ as the image of $\mathbb{R}_{\geq 0} \times \text{SO}(3)$. We do this by associating each element (a, q) , $a \geq 0$, $q = (q_1, q_2, q_3)$ with the symmetric map $\tilde{\Sigma} \in \text{Sym}^+ T_{q_3} S^2$ such that

$$\tilde{\Sigma} q_1 = e^{2a} q_1, \quad \tilde{\Sigma} q_2 = e^{-2a} q_2.$$

- (2) We generate a 'lattice' of comparison points on S^2 . This points set only has to be generated once, and can then be reused for any dataset. Choose $a_{\max} > 0$ and $n_a \in \mathbb{N}$ and define

$$a_l = \frac{l}{n_a} a_{\max}, \quad \alpha_l = \sqrt{e^{2a_l} - e^{-2a_l}}, \quad T_{\max, l} = 2\pi e^a, \quad l = 0, 1, \dots, n_a.$$

The value $T_{\max, l}$ is chosen so that the geodesic going along the eigenvector of e^{-a} from the north pole has time to reach the south pole. Next, for a chosen $n_\psi, n_T \in \mathbb{N}$, and for $i = 1, \dots, n_\psi$, $j = 1, \dots, n_R$, define

$$T_{j, l} = \frac{j}{n_T} T_{\max, l}, \quad \psi_i = \frac{i}{n_\psi} \pi, \quad k_i = \sin^{-1}(\psi_i/2).$$

Finally, we define

$$\begin{aligned} v_{i, j, l}(t) &= e^{a_l} \text{dn}(K(k_i) + \alpha_l(T_{j, l} - t), k_i), \\ w_{i, j, l}(t) &= e^{-a_l} k_i \text{sn}(K(k_i) + \alpha_l(T_{j, l} - t), k_i) \end{aligned}$$

Let $N = (0, 0, 1)^\dagger$ be the north pole and let $\Sigma'_l \in \text{Sym}^+ T_N S^2$ be the symmetric endomorphism with eigenvalue e^{2a_l} and e^{-2a_l} in respectively the directions $(1, 0, 0)^\dagger$ and $(0, 1, 0)^\dagger$. Define $q(t) = q_{i, j, l}(t)$ in $\text{SO}(3)$ as solutions of

$$q(t)^{-1} \dot{q}(t) = \begin{pmatrix} 0 & 0 & v_{i, j, l}(t) \\ 0 & 0 & w_{i, j, l}(t) \\ -v_{i, j, l}(t) & -w_{i, j, l}(t) & 0 \end{pmatrix}, \quad q(0) = 1_3.$$

Finally, define $z_{i, j, l} = q_{i, j, l}(T_{j, l})N$ and for $i > 0$, define its mirror in the y, z -axis, $z_{\pm i, \pm j, l} = \text{diag}\{\pm 1, \pm 1, 1\} z_{i, j, l}$. Then $z_{i, j, l}$ are all endpoints of most probable paths with length $T_{j, l}$.

In summary, we need to solve $(n_a + 1) \times n_\psi \times n_T$ -ODEs in $\text{SO}(3)$. We will use the data $z_{i, j, l}$, $T_{j, l}$, a_l in what follows.

- (3) We use the previous data to make a an approximation to $d_\rho(\pi^{-1}(y), (N, \Sigma_l))$. We have a bound

$$d(\pi(y), (N, \Sigma_l)) \leq T_{j, l} + e^{a_l} \cos^{-1}(y^\dagger z_{i, j, l}),$$

from the fact that the most probable path in the direction of the eigenvalue e^{-a_l} is the slowest moving in the Riemannian metric. Define a function

$$\text{Dist}_l(y) = \min_{\substack{i=0, \pm 1, \dots, \pm m_1 \\ j=1, \dots, m_2}} (T_{j, l} + e^{a_l} \cos^{-1}(y^\dagger z_{i, j, l})), \quad y \in S^2.$$

- (4) Finally, find we define $q' \in \mathbb{R} \times \text{O}(3)$ as the element corresponding to the best choice Σ' by

$$l' \times q' = \underset{\substack{l=0,1,\dots,n_a \\ q \in \text{O}(3)}}{\text{argmin}} \sum_{r=1}^n \text{Dist}_l(q^{-1}y_r)^2.$$

This can be done by using an optimizer in q or optimizing over a grid $n_1 \times n_2 \times n_3$ of $\{q'_{i,j,k} : i = 1, \dots, n_1, j = 1, \dots, n_2, k = 1, \dots, n_3\}$, where

$$q'_{i,j,k} = \begin{pmatrix} \cos(\frac{2\pi i}{n_1-1}) & \sin(\frac{2\pi i}{n_1-1}) & 0 \\ -\sin(\frac{2\pi i}{n_1-1}) & \cos(\frac{2\pi i}{n_1-1}) & 0 \\ 0 & 0 & 1 \end{pmatrix} \begin{pmatrix} \cos(\frac{2\pi j}{n_2-1}) & 0 & \sin(\frac{2\pi j}{n_2-1}) \\ 0 & 0 & 0 \\ -\sin(\frac{2\pi j}{n_2-1}) & 0 & \cos(\frac{2\pi j}{n_2-1}) \end{pmatrix} \begin{pmatrix} 1 & 0 & 0 \\ 0 & \cos(\frac{2\pi k}{n_3-1}) & \sin(\frac{2\pi k}{n_3-1}) \\ 0 & -\sin(\frac{2\pi k}{n_3-1}) & \cos(\frac{2\pi k}{n_3-1}) \end{pmatrix}.$$

8.2. General geometries. For general Riemannian manifolds, the system (5.5) can be solved numerically by integrating $v(t)$, $f(t)$ and $\chi(t)$ forward and solving for $\chi(T) = 0$. Algorithm 1 shows a simple gradient-based approach for finding most probable paths from a starting point $\Sigma \in \text{Sym}^+ T_x M$ to $y \in M$.

Algorithm 1: Most probable path from Σ to y

Data: $S \in \text{Sym}^+ \mathbb{R}^d$, $y \in M$, $f^x \in O(TM)$, $T, \delta > 0$

Result: $v(0), \chi(0)$ s.t. $d(\gamma(T), y)^2 + \|\chi(T)\|^2 \leq \delta$

while $d(\gamma(T), y)^2 + \|\chi(T)\|^2 > \delta$ **do**

1. numerically integrate forward $\gamma(t)$ and $\chi(t)$
2. compute gradient $g(v(0), \chi(0)) \leftarrow \nabla_{v(0), \chi(0)} (d(\gamma(T), y)^2 + \|\chi(T)\|^2)$
3. update initial conditions: $(v(0), \chi(0)) \leftarrow (v(0), \chi(0)) - \epsilon g(v(0), \chi(0))$

end

The deviation $d(\gamma(T), y)$ between the endpoint $\gamma(T)$ and the target y can be replaced by, for example, the Euclidean distance in a chart or using an embedding of M .

The gradients of $d(\gamma(T), y)^2$ and $\|\chi(T)\|^2$ with respect to the initial conditions $v(0)$ and $\chi(0)$ can be derived by solving the adjoint of (5.5). This can be achieved directly using automatic differentiation frameworks that implement the adjoint equations implicitly with reverse automatic differentiation. In practice, the gradient-descent algorithm above can be replaced by quasi-Newton methods such as BFGS to improve convergence.

Figure 1 shows examples of most probable paths on sphere S^2 and the hyperbolic space H^2 computed using Algorithm 1, and with derivatives computed using the Jax automatic differentiation framework [1], implemented in the JaxGeometry¹ package.

¹<https://bitbucket.org/stefansommer/jaxgeometry>

8.3. Mean and covariance estimation. Given i.i.d. samples y_1, \dots, y_n , the mean and covariance estimator (2.6) can in general be found by solving the constrained minimization problem

$$(8.1) \quad \begin{aligned} & \underset{\Sigma \in \text{Sym}^+ TM, (v_1(0), \chi_1(0)), \dots, (v_n(0), \chi_n(0))}{\text{argmin}} \sum_{j=1}^n \left(v_j(0)^T S^{-2} v_j(0) + \ln \det_g \Sigma \right) \\ & \text{s.t. } (\gamma(T) = y_1, \chi_1(T) = 0), \dots, (\gamma(T) = y_n, \chi_n(T) = 0) \end{aligned}$$

where $\gamma_i(t), \chi_i(t)$ are the trajectories defined by (5.1) with initial conditions $v_i(0), \chi_i(0)$.

Let $F : \text{Sym}^+ TM \times (\mathbb{R}^d \times \wedge^2 \mathbb{R}^d)^{\times n} \rightarrow \mathbb{R}$ denote the objective function of (8.1). The velocities $v_i(0)$ on which F is evaluated in (8.1) depend on Σ . Let $G : \text{Sym}^+ TM \times \mathbb{R}^d \times \wedge^2 \mathbb{R}^d \rightarrow \mathbb{R}^d \times \wedge^2 \mathbb{R}^d$ denote a map $\Sigma, v, \chi \mapsto \begin{pmatrix} \gamma(T) - v \\ \chi(T) \end{pmatrix}$ encoding the constraints such that $G(\Sigma, v_i(0), \chi_i(0)) = 0$, for example using a chart around v to express the end-point difference $\gamma(T) - v$. The inverse function theorem implies that

$$(8.2) \quad D_\Sigma v_i(0) = -\left(D_{v, \chi} G|_{\Sigma, v_i(0), \chi_i(0)}\right)^{-1} D_\Sigma G|_{\Sigma, v_i(0), \chi_i(0)}.$$

Thus, an infinitesimal change $\delta \Sigma$ of Σ results in the variation

$$(8.3) \quad \begin{aligned} \delta F &= \nabla_\Sigma F \delta \Sigma + \sum_{i=1}^n \nabla_{v_i} F D_\Sigma v_i(0) \delta \Sigma \\ &= \nabla_\Sigma F \delta \Sigma - \sum_{i=1}^n \nabla_{v_i} F \left(D_{v, \chi} G|_{\Sigma, v_i(0), \chi_i(0)} \right)^{-1} D_\Sigma G|_{\Sigma, v_i(0), \chi_i(0)} \delta \Sigma. \end{aligned}$$

This leads to the iterative procedure for solving (8.1) listed in Algorithm 2.

Algorithm 2: Most likely Σ for observation y_1, \dots, y_n .

Data: $y_1, \dots, y_n \in M$, $f^x \in O(TM)$, $T, \delta > 0$

Result: Σ (locally) minimizing (8.1)

while $\max(\|\nabla_\Sigma F\|, \|\nabla_{(v_1, \chi_1)} \|G\|^2, \dots, \|\nabla_{(v_n, \chi_n)} \|G\|^2\|) > \delta$ **do**

1. for $i = 1, \dots, n$, numerically integrate forward $\gamma_i(t)$ and $\chi_i(t)$
2. compute $\nabla_\Sigma F$, $D_{(v_i, \chi_i)} G$, $\|\nabla_{(v_i, \chi_i)} \|G\|^2\|$
3. update Σ : $\Sigma \leftarrow \Sigma - \epsilon(\nabla_\Sigma F + \sum_{i=1}^n \nabla_{v_i} F D_\Sigma v_i(0))$
4. update $(v_i(0), \chi_i(0))$: $(v_i(0), \chi_i(0)) \leftarrow (v_i(0), \chi_i(0)) - \epsilon \nabla_{(v_i, \chi_i)} \|G\|^2$

end

The right-hand side of (8.2) is in Algorithm 2 evaluated at the current guess for $(v_i(0), \chi_i(0))$ and hence provides only an approximation to the true derivative. This implies that the stability of the algorithm can increase by taking multiple update steps for the initial conditions $(v_i(0), \chi_i(0))$ for each update step for Σ . The convergence rate can in addition be increased by using e.g. descent-schemes with momentum such as the ADAM optimizer instead of pure gradient descent.

Figure 5 show examples of estimation of Σ on the sphere S^2 , T^2 and H^2 using Algorithm 2.

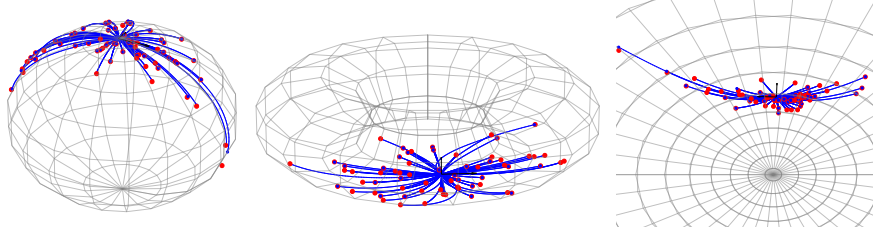


FIGURE 5. Mean and covariance estimation on the sphere S^2 and the embedded torus T^2 using Algorithm 2. Blue curves shows MPPs from the estimated mean to the 64 samples (red points).

APPENDIX A. DEFINITION OF SUB-RIEMANNIAN GEOMETRY

We give a quick introduction to sub-Riemannian geometry and refer to [10] for details. A sub-Riemannian manifold is a triple (M, E, ρ) where M is a connected manifold, E is a subbundle of the tangent bundle TM and $\rho = \langle \cdot, \cdot \rangle_\rho$ is a metric tensor defined only on E . This tensor defines a vector bundle morphism $\sharp^\rho : T^*M \rightarrow E \subseteq TM$ given by

$$\alpha(v) = \langle \sharp^\rho \alpha, v \rangle_\rho.$$

Consequently, we obtain a positive semi-definite symmetric tensor $\rho^* = \langle \cdot, \cdot \rangle_{\rho^*}$ on T^*M defined by

$$\langle \alpha, \beta \rangle_{\rho^*} = \langle \sharp^\rho \alpha, \sharp^\rho \beta \rangle_\rho.$$

This tensor degenerates along the subbundles $\text{Ann}(E) \subseteq T^*M$ of covectors vanishing on E . It follows that a sub-Riemannian manifold can equivalently be defined as a connected manifold with positive, semi-definite cometric ρ^* that degenerates along a subbundle.

An absolutely continuous curve $\gamma : [0, T] \rightarrow M$ is called *horizontal* if $\dot{\gamma}(t) \in E_{\gamma(t)}$ for almost every t . For such a curve, we define its length to be

$$L^\rho(\gamma) = \int_0^T |\dot{\gamma}|_\rho(t) dt.$$

This length is invariant under reparametrization, so we can restrict our considerations to the case $T = 1$.

For any $x, y \in M$, we define

$$d_\rho(x, y) = \inf \left\{ L^\rho(\gamma) : \begin{array}{l} \gamma : [0, 1] \rightarrow M \text{ horizontal} \\ \gamma(0) = x, \gamma(1) = y \end{array} \right\}.$$

We notice that if there are no horizontal curves connecting the two points, then $d_\rho(x, y) = \infty$. Let $x \in M$ be a given point. We define $\mathcal{C}(x)$ as the space of all horizontal curves defined on $[0, 1]$, with L^2 -derivative, that start in x . This collection has a natural structure of a Hilbert manifold, see [10, Chapter 5.1] for details. Define a mapping

$$\Pi : \mathcal{C}(x) \rightarrow M, \quad \gamma \mapsto \gamma(1).$$

Define $\mathcal{C}(x, y) = \Pi^{-1}(y)$. A point $\gamma \in \mathcal{C}(x, y)$ is called *regular* if $\Pi_{*, \gamma} : T_\gamma \mathcal{C}(x) \rightarrow T_y M$ is surjective. Otherwise, γ is called *singular* or *abnormal* curves.

Assume that $\mathcal{C}(x, y)$ non-empty. Define $F : \mathcal{C}(x, y) \rightarrow \mathbb{R}$ by $\gamma \mapsto L^\rho(\gamma)$. We look at minimal elements in $\mathcal{C}(x, y)$ with respect to F . If γ is a regular curve, then $\mathcal{C}(x, y)$

locally has the structure of a Hilbert manifold around γ by the inverse function theorem. Hence, any regular minimal element must be a critical, i.e. we must have $F_{*,\gamma} = 0$. Such curves are called *normal geodesics*, and will always be locally length minimizing. It can be shown that all such curves, up to reparametrization, be found as a projecting of a solution of a Hamiltonian system. The Hamiltonian is given by

$$P(\alpha) = \frac{1}{2} \langle \alpha, \alpha \rangle_{\rho^*}, \quad \alpha \in T^*M.$$

In conclusion, length minimizers are either normal geodesics or abnormal curves. These classes of curves are not necessarily disjoint.

We say that E is bracket-generating if for every point $x \in M$,

$$\text{span}\{X_i, [X_i, X_j], [X_i, [X_j, X_k]], \dots\}|_x \in T_x M, \quad X_i \in \Gamma(E),$$

that is, if sections of E generate the entire tangent bundle TM . If this condition holds, then any pair of points can be connected by a horizontal curve. The value of d_ρ is always finite, and furthermore, it induces the same topology as the manifold topology.

Remark A.1. Let L be a second order operator on M without constant term, such that for any pair of smooth functions $f, g \in C^\infty(M)$,

$$L(fg) - fLg - gLf = \langle df, dg \rangle_{\rho^*}.$$

In other words, locally, L can always be written as $L = \sum_{j=1}^{\text{rank } E} V_j^2 + V_0$, where $V_1, \dots, V_{\text{rank } E}$ is a local orthonormal basis of (E, ρ) . If E is bracket generating, then L is hypoelliptic [7] and its heat semigroup $p_t(x, y)$ has a strictly positive density [19].

APPENDIX B. SUB-RIEMANNIAN NORMAL GEODESICS ON $(\text{Sym}^+ TM, E, \rho)$

By the discussion in Section 4.2, it follows that we can write a normal geodesic as $\Sigma(t) = f(t)^{-1} S^2 f(t)$ where $f(t)$ is a normal geodesic in $(O(TM), \mathcal{H}, \rho_S)$. We do the computations here.

Recall the definition of the vector fields H_a , $a \in \mathbb{R}^n$ and ξ_A , $A \in \mathfrak{so}(n)$ in Section 3. We introduce corresponding Hamiltonian functions

$$P_a(\alpha) = \alpha(H_a), \quad Q_A(\alpha) = \alpha(\xi_A), \quad \alpha \in T^*O(TM).$$

Our formulas in (3.3), then give corresponding relations in terms of Poisson brackets

$$\{P_a, P_b\} = -Q_{\underline{R}(a,b)}, \quad \{Q_A, P_a\} = P_{Aa}, \quad \{Q_A, Q_B\} = Q_{[A,B]}.$$

Since $H_{Se_1}, \dots, H_{Se_d}$ is a global orthonormal basis, we have that the sub-Riemannian Hamiltonian is given by

$$P = \frac{1}{2} \sum_{j=1}^d P_{Se_j}^2.$$

Let $\lambda(t) = e^{t\bar{P}}(\lambda_0)$ be a solution in T^*FM along $f(t)$ in FM and define curves $v(t)$ in \mathbb{R}^d and $A(t)$ in $\mathfrak{so}(d)$ by

$$P_a(t) = P_a(\lambda(t)) = \langle S^{-2}v(t), a \rangle, \quad Q_B(t) = Q_B(\lambda(t)) = \langle A(t), B \rangle.$$

Then along a solution, we have

$$\langle S^{-2}\dot{v}, a \rangle = \dot{P}_a = \{P_a, P\} = - \sum_{j=1}^d P_{Se_j} Q_{\underline{R}(a, Se_j)} = - \sum_{j=1}^d \langle S^{-2}v, Se_j \rangle \langle A, \underline{R}(a, Se_j) \rangle$$

$$\begin{aligned}
&= \sum_{j=1}^d \langle S^{-1}v, e_j \rangle \langle \underline{R}(A)Se_j, a \rangle = \langle \underline{R}(A)v, a \rangle \\
\langle \dot{A}(t), B \rangle &= \dot{Q}_B = \{Q_B, P\} = \sum_{j=1}^d P_{Se_j} P_{BSe_j} = \sum_{j=1}^d \langle S^{-2}v, Se_j \rangle \langle BSe_j, S^{-2}v \rangle \\
&= \langle Bv, S^{-2}v \rangle = \langle v \wedge S^{-2}v, B \rangle.
\end{aligned}$$

In summary, $\dot{v} = S^2 \underline{R}(A)v$ and $\dot{A} = v \wedge S^{-2}v$.

Let $\beta \in \Gamma(T^* \mathcal{O}(TM))$ be a one-form on $\mathcal{O}(TM)$ and define the corresponding vertical lift $\text{vl } \beta \in \Gamma(T(T^* \mathcal{O}(TM)))$ by

$$\text{vl } \beta|_{\alpha} = \frac{d}{dt}(\alpha + t\beta_f)|_{t=0}, \quad \alpha \in T_f^* \mathcal{O}(TM).$$

Let ϑ be the Liouville one form $\vartheta|_{\alpha} = \pi^* \alpha$ with canonical symplectic form $\sigma = -d\vartheta$. Observe that $\sigma(\text{vl } \beta, \cdot) = -(\pi^* \beta)(\cdot)$. Then

$$dP(\text{vl } \beta) = \sum_{j=1}^d P_{Se_j} \beta(H_{Se_j}) = \sigma(\vec{P}, \text{vl } \beta) = \beta(\pi_* \vec{P}).$$

If we consider this along the curve, we have

$$\begin{aligned}
\sum_{j=1}^d P_{Se_j} \beta(H_{Se_j})|_{\lambda(t)} &= \sum_{j=1}^d \langle S^{-1}v(t), e_j \beta(H_{Se_j})|_{f(t)} \rangle = \beta(H_{v(t)})|_{f(t)} \\
&= \beta(\pi_* \vec{P})|_{\lambda(t)} = \beta(\dot{f}(t))
\end{aligned}$$

It follows that

$$\dot{f}(t) = H_{v(t)}, \quad \dot{v}(t) = S^2 \underline{R}(f(t))(A(t))v(t), \quad \dot{A}(t) = v(t) \wedge S^{-2}v(t).$$

We see that these are exactly the equations of found in the proof of Theorem 5.1 without the condition $A(T) = 0$.

REFERENCES

- [1] J. Bradbury, R. Frostig, P. Hawkins, M. J. Johnson, C. Leary, D. Maclaurin, G. Necula, A. Paszke, J. VanderPlas, S. Wanderman-Milne, and Q. Zhang. JAX: Composable transformations of Python+NumPy programs, 2018.
- [2] K. Engø, A. Marthinsen, and H. Z. Munthe-Kaas. The diffman package on github. <https://github.com/kenthe/DiffMan>. Accessed: 2021-10-19.
- [3] M. Frechet. Les éléments aléatoires de nature quelconque dans un espace distancié. *Ann. Inst. H. Poincaré*, 10:215–310, 1948.
- [4] T. Fujita and S.-i. Kotani. The Onsager-Machlup function for diffusion processes. *Journal of Mathematics of Kyoto University*, 22(1):115–130, 1982.
- [5] P. Hansen, B. Eltzner, S. F. Huckemann, and S. Sommer. Diffusion Means in Geometric Spaces. *arXiv:2105.12061*, May 2021.
- [6] P. Hansen, B. Eltzner, and S. Sommer. Diffusion Means and Heat Kernel on Manifolds. *Geometric Science of Information 2021*, Feb. 2021.
- [7] L. Hörmander. Hypoelliptic second order differential equations. *Acta Math.*, 119:147–171, 1967.
- [8] E. P. Hsu. *Stochastic analysis on manifolds*, volume 38 of *Graduate Studies in Mathematics*. American Mathematical Society, Providence, RI, 2002.
- [9] P. Malliavin. Stochastic calculus of variation and hypoelliptic operators. In *Proceedings, International Symposium on SDE, Kyoto*, 1976.

- [10] R. Montgomery. *A tour of subriemannian geometries, their geodesics and applications*, volume 91 of *Mathematical Surveys and Monographs*. American Mathematical Society, Providence, RI, 2002.
- [11] X. Pennec. Intrinsic Statistics on Riemannian Manifolds: Basic Tools for Geometric Measurements. *J. Math. Imaging Vis.*, 25(1):127–154, 2006.
- [12] R. W. Sharpe. *Differential geometry*, volume 166 of *Graduate Texts in Mathematics*. Springer-Verlag, New York, 1997. Cartan’s generalization of Klein’s Erlangen program, With a foreword by S. S. Chern.
- [13] I. Shigekawa. On stochastic horizontal lifts. *Z. Wahrsch. Verw. Gebiete*, 59(2):211–221, 1982.
- [14] S. Sommer. Anisotropic Distributions on Manifolds: Template Estimation and Most Probable Paths. In *Information Processing in Medical Imaging*, volume 9123 of *Lecture Notes in Computer Science*, pages 193–204. Springer, 2015.
- [15] S. Sommer. Evolution Equations with Anisotropic Distributions and Diffusion PCA. In F. Nielsen and F. Barbaresco, editors, *Geometric Science of Information*, number 9389 in *Lecture Notes in Computer Science*, pages 3–11. Springer International Publishing, 2015.
- [16] S. Sommer. Anisotropically Weighted and Nonholonomically Constrained Evolutions on Manifolds. *Entropy*, 18(12):425, Nov. 2016.
- [17] S. Sommer. An Infinitesimal Probabilistic Model for Principal Component Analysis of Manifold Valued Data. *Sankhya A*, Aug. 2018.
- [18] S. Sommer and A. M. Svane. Modelling anisotropic covariance using stochastic development and sub-Riemannian frame bundle geometry. *Journal of Geometric Mechanics*, 9(3):391–410, June 2017.
- [19] D. W. Stroock and S. R. S. Varadhan. On the support of diffusion processes with applications to the strong maximum principle. In *Proceedings of the Sixth Berkeley Symposium on Mathematical Statistics and Probability (Univ. California, Berkeley, Calif., 1970/1971)*, Vol. III: *Probability theory*, pages 333–359. Univ. California Press, Berkeley, Calif., 1972.

UNIVERSITY OF BERGEN, DEPARTMENT OF MATHEMATICS, P.O. BOX 7803, 5020 BERGEN, NORWAY

Email address: `erlend.grong@uib.com`

UNIVERSITY OF COPENHAGEN, UNIVERSITETSPARKEN 5, CK-2100 COPENHAGEN E, DENMARK

Email address: `sommer@di.ku.dk`